Environmental Earth Sciences (2020) 79:494
https://doi.org/10.1007/s12665-020-09246-2

ORIGINAL ARTICLE

Scenarios to control land subsidence using numerical modeling of groundwater exploitation: Aliabad plain (in Iran) as a case study

Ali Edalat[1] · Mahdi Khodaparast[1] · Ali M. Rajabi[2]

Received: 2 June 2020 / Accepted: 14 October 2020 / Published online: 27 October 2020

Abstract
The unconfined aquifer beneath the Aliabad plain is one of the few freshwater resources in northwestern Qom province in Iran. Land subsidence in the Aliabad plain is primarily the result of extensive overexploitation of groundwater resources and successive droughts. The harmful effects of overexploitation include significant socioeconomic consequences and severe damage to aquifers. The current study proposes an accurate scenario model that reduces the overall land subsidence by assessing different scenarios for future groundwater exploitation in the plain. The quantitative model consists of 120 time-steps over a period of 10 years (2006–2016). Model validation was achieved by comparing the calculated groundwater level variations with the results of piezometric evaluations in modeling. The results of the validated model were used to predict variations in the aquifer hydraulic head caused by changes in exploitation under different scenarios. Modeling of the Aliabad plain revealed that a 10% decrease in pumping will reduce and stabilize the groundwater decline and a 30% reduction will help recharge the aquifer. The model simulation was able to predict critical land subsidence of 35 cm by 2016. The geometric location of maximum land subsidence was predicted by comparing the geometric distribution of predicted land subsidence patterns with subsidence results from radar interferometry. Prediction of land subsidence by 2026 indicated that management of the exploitation of resources and strict aquifer stabilization programs can reduce the damage to the aquifer.

Keywords Aliabad plain · Qom province · Groundwater · Land subsidence · Numerical modeling

Introduction

Excessive exploitation of groundwater resources will increase the effective stress and the consequent compression of fine-grained sediment and cause subsidence of the aquifer system (Terzaghi 1925). Subsidence is the collapse or settlement of the ground surface (Galloway and Burbey 2011) which can have negative consequences such as the formation of ground fissures (Budhu 2011), an increased flooding potential (Rodolfo and Siringan 2006), alterations in soil morphology (Moe et al. 2017) and damage to underground infrastructures (Bell 1981). Ground subsidence due to persistent and large-scale extraction of groundwater which produces a significant decrease in the groundwater level of an aquifer has been reported in many locations (Bajni et al. 2019; Hu et al. 2019; Ma et al. 2019).

In Iran, subsidence has been reported in many areas, including Rafsanjan (Rahnama and Moafi 2009), Mashhad (Motagh et al. 2007), Yazd (Amighpey and Arabi 2016), Arak (Rajabi and Ghorbani 2016), and Tehran (Dehghani et al. 2013; Mahmoudpour et al. 2016). Effective management of groundwater resources is essential to mitigate the negative effects of subsidence (Konikow and Kendy 2005). Groundwater modeling is an essential tool for managing water resources in aquifers. These models can be used to estimate hydraulic parameters and predict changes in an aquifer which can change in response to weather fluctuations and pumping (Regli et al. 2003).

Numerical techniques provide flexible and powerful approaches for solving issues regarding groundwater flow modeling, such as the intrinsic complexities of aquifer

✉ Mahdi Khodaparast
khodaparast@qom.ac.ir

Ali Edalat
a.edalat@stu.qom.ac.ir

Ali M. Rajabi
amrajabi@ut.ac.ir; amrajabi@ymail.com

[1] Department of Civil Engineering, University of Qom, Qom, Iran

[2] Department of Engineering Geology, University of Tehran, Tehran, Iran

systems, heterogeneous multilayer tables and inaccurate input information in complicated field situations (Bakker and Hemker 2004). A variety of software packages have been created for numerical modeling of groundwater (Diersch 2005). One of these is MODFLOW, which uses the finite difference method to solve flow equations (McDonald and Harbaugh 1988). Software packages such as the Groundwater Modeling System (GMS), Visual MODFLOW and Processing MODFLOW for Windows (PMWIN) use MODFLOW architecture (Chiang 2005). The subsidence and aquifer-system compaction package (SUB) is a subprogram of MODFLOW which is used to simulate drainage, changes in storage resources, and the density of aquifer layers. This package can create a binary vertical displacement project in GSM that can be shown as a dataset (Hoffmann et al. 2003).

Researchers have simulated groundwater depletion and subsidence for different aquifers in Iran. Karimipour and Rakhshanderoo (2011) and Mahdavi et al. (2013) simulated the hydraulic behavior of the Shiraz plain and the Hamedan aquifer, respectively, using PMWIN software. Lashkaripour and Ghafoori (2011) investigated the effect of a drop in water level in the aquifer under Torbat-e-jam plain. Their results showed that an increase in groundwater discharge compared to recharge caused the drop in the water level and worsened the quality of the groundwater in most regions of the plain. Mahmoudpour et al. (2016) simulated the subsidence caused by a decrease in the groundwater level in the plain southwest of Tehran. Their results confirmed that soil subsidence due to groundwater pumping is a significant threat to the area.

Cui et al. (2014) performed numerical modeling of groundwater and subsidence in Tianjin plain using MODFLOW 2005 and land SUB. The results showed that the level of groundwater could gradually increase with a decrease in groundwater withdrawal, which would lead to a subsequent decrease in the rate of land subsidence in this area. Qin et al. (2018) provided a numerical model of groundwater and subsidence in Beijing plain by assessing the rate of land subsidence under different scenarios to decrease groundwater pumping by engaging in sustainable economic development. Karimi et al. (2019) examined changes in the Tehran groundwater aquifer using MODFLOW. The results showed adequate agreement between the observed and calculated hydraulic heads.

Aliabad plain is located in the Saveh basin in both Qom and Markazi provinces in central Iran (Fig. 1). In recent years, the increased groundwater discharge from the Aliabad plain aquifer caused by increased demand for agricultural and drinking water has reduced the groundwater level and, consequently, subsidence has occurred in a broad area of the plain. Despite the importance of land subsidence in Aliabad plain, limited studies have been done in this regard. Rajabi (2018) numerically studied subsidence of Aliabad plain from 2001 to 2013 using PLAXIS software. The results showed that the plain experienced up to 76 cm of subsidence over the 12-year period.

The primary purpose of the present study has been to simulate and predict the groundwater level in the Aliabad plain aquifer. The model will be used to estimate the hydraulic parameters and predict future changes in the aquifer. Changes in the groundwater level in the Aliabad plain aquifer from 2006 to 2016 have been modeled and the hydraulic head has been simulated using GMS.

After validation of the model, the groundwater changes and land deformation up to 2026 were studied under the following three scenarios: maintaining the current rate of discharge, decreasing the rate by 10%, and decreasing the rate by 30%. The results were used to predict how a change in pumping alters the plain groundwater level and suggested the best scenario for minimizing the total subsidence. The model provides a scientific basis for the development and management of groundwater resources in this area. Insufficiency of reliable data for the sake of modeling and the intrinsic complexity of the subsidence phenomenon caused by excessive extraction of groundwater including gradual progression, tremendous vastness and inhomogeneous progression pattern gave rise to a number of limitations to study this phenomenon. In this study, as the research novelty, a special process has been adopted by which with respect to the aforementioned limitations, a model with adequate efficiency could be prepared which is able to predict future behavior of the aquifer under different scenarios of water resources exploitation.

Study region

Aliabad plain is about 1794 km^2 in size and is located in northwestern Qom province. It covers part of the Saveh aquifer (Fig. 1). The annual temperature of the plain ranges from 5 to 31 °C. The mean annual precipitation and evaporation rates on the plain are 185 and 2849 mm, respectively. Most parts of the plain have experienced land subsidence caused by excess groundwater exploitation (Edalat et al. 2020). The Qarah-Chay river is the only permanent river in the region and the Mazlaghan river flows into it. After the draining of the Saveh dam in 1992, the entrance of the Qarah-Chay river into the aquifer was disrupted. Thus, over the last decade, downstream farmers have used groundwater to supply agricultural water, which has caused subsidence from a drop in water level in the aquifer (Edalat et al. 2020).

Studies on the groundwater of Aliabad plain have shown that the region is underlain by an unconfined aquifer with an area of 1630 km^2. The region under study is located in the southern portion of the plain and falls entirely in Qom province (Fig. 1c). This region was selected because of existing reliable information as well as signs of progressive subsidence,

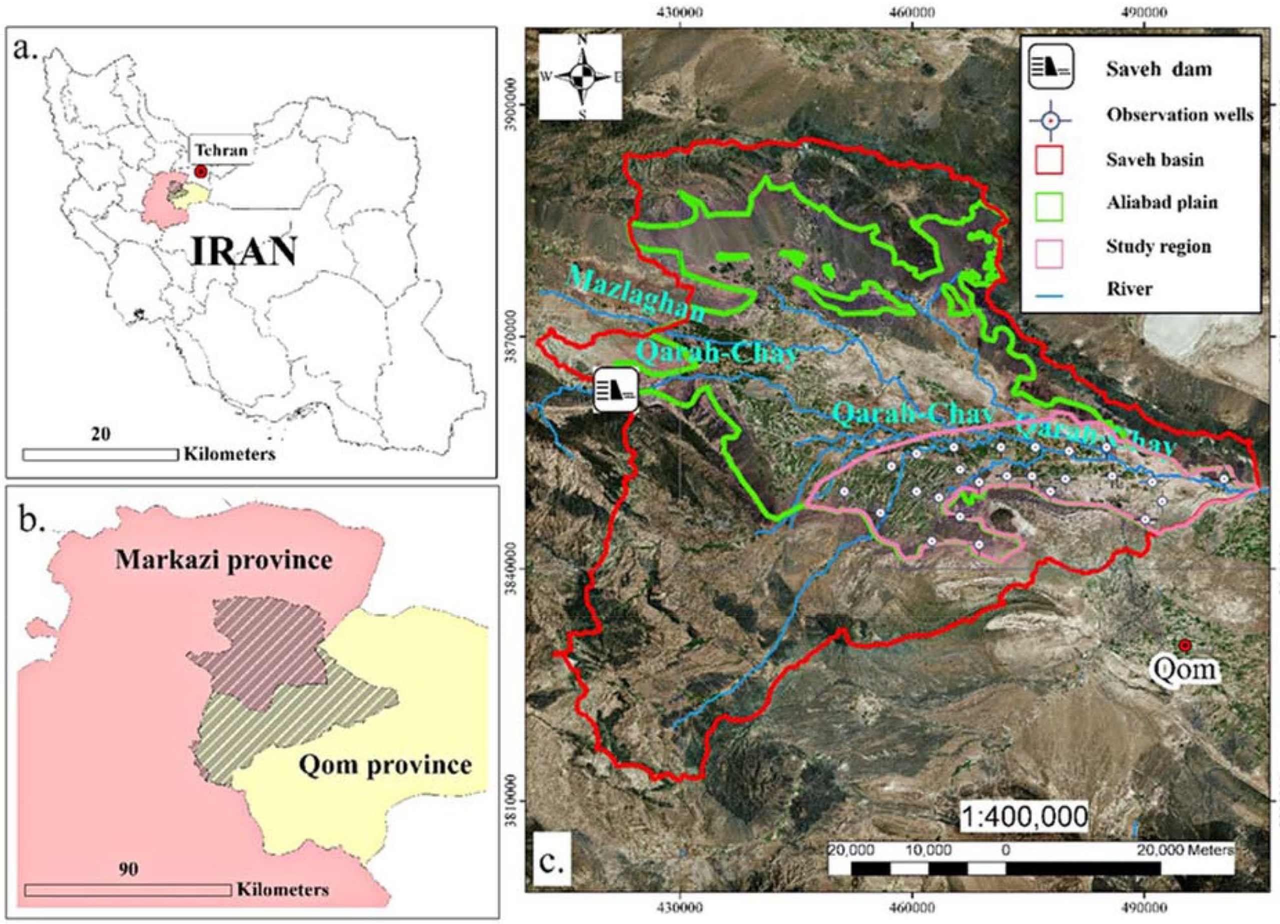

Fig. 1 **a** Locations of Markazi and Qom provinces in Iran, **b** location of Saveh basin in provinces of Markazi and Qom and location of Aliabad plain in Saveh basin, and **c** location of the studied region in Aliabad plain and location of observation wells in the studied area

such as cracks on walls and in piping. Figure 1c shows the locations of 26 observation wells that are active in the region (Qom Regional Water Company 2000).

Research method

The hydraulic properties and land deformation data provided by satellite images were used to model the groundwater. The input parameters of the groundwater model underwent steady and unsteady calibration, then were corrected and were found to be close to the observed data. Aquifer deformation has been predicted using the subsidence prediction package.

Collection and evaluation of basic information

Geological and hydraulic properties

The alluvial sediment in Aliabad plain is primarily from sedimentation from existing rivers. Moving from east to west on the plain, river discharge decreases and the alluvial sediment becomes fine grained. The geological materials that underlie the Aliabad plain chiefly consist of loose sediments such as silts and clays and, at high altitudes, of conglomerates with microconglomerate mid-layers.

There are no traces of a major fault in the plain (Edalat et al. 2020). Figure 2a shows the depth of the sediment in the region. The maximum and minimum bedrock heights are 20 and 300 m, respectively (Qom Regional Water Company 2000). Information from the observation wells was obtained from the regional water company (Qom Regional Water Company 2016) and was used to plot groundwater levels (Fig. 2b) and isobath maps (Fig. 2c). As seen in Fig. 2b, the elevation of the groundwater potentiometric surface in the area ranges from 810 to 930 m above sea level (asl). Figure 2c shows that the groundwater depth in the area ranges from 10 to 130 m. Figure 2d shows the transmissivity contour lines (Qom Regional Water Company 2000). The values of transmissivity vary from 100 m^2/day at the border of the study area to 3000 m^2/day at the Qarah-Chay riverbank.

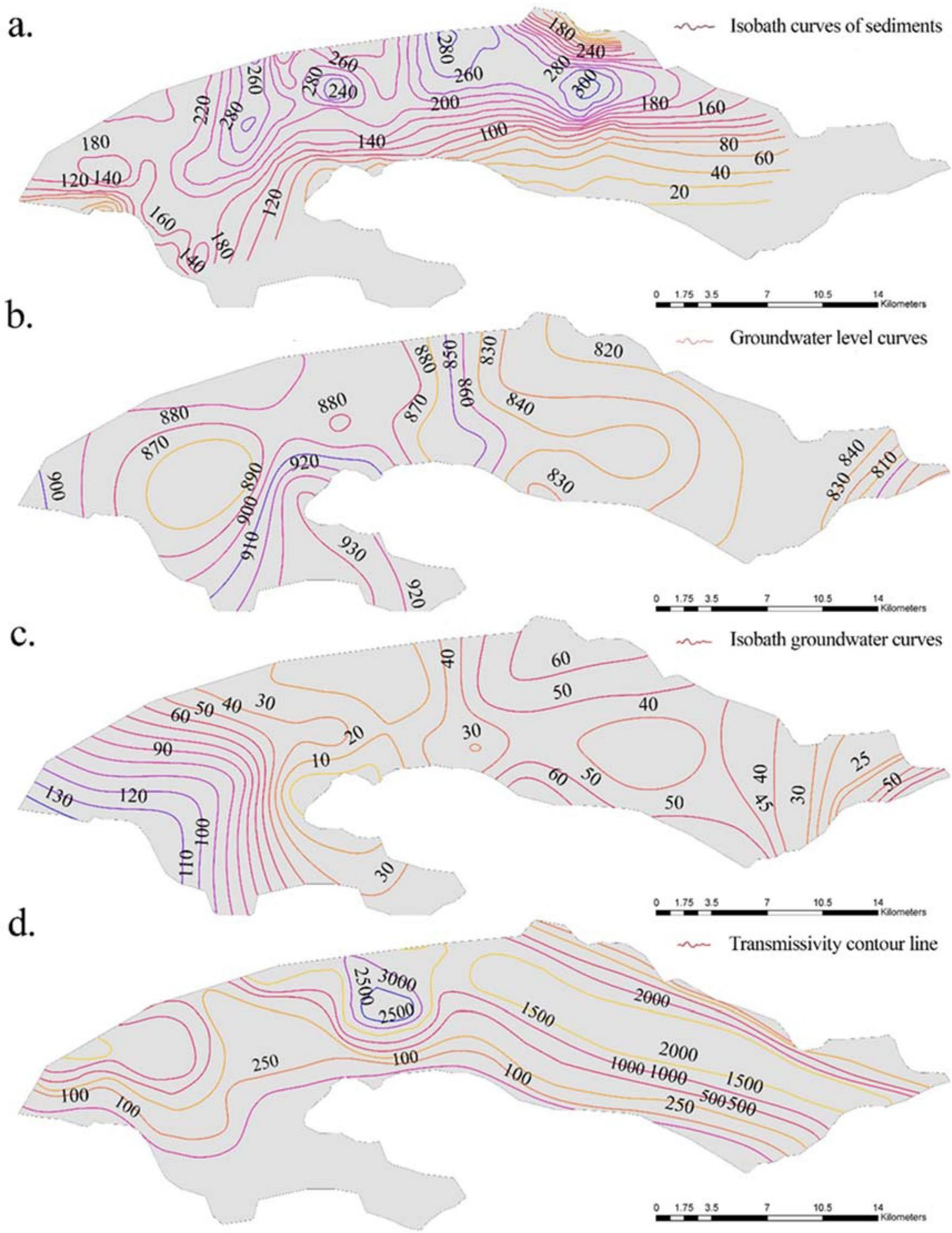

Fig. 2 **a** Isobath curves of sediments in the area of interest, **b** groundwater level curves in Aliabad plain, **c** isobath groundwater curves in the area, and **d** transmissivity contour line in the area

Figure 3 shows the volume of each recharge and discharge components for the water balance of the aquifer. As seen, the total volumes of the recharge and withdrawal components of the aquifer are 521.37 and 609.54 million m^3, respectively. These figures indicate a shortage of 88.17 million m^3 per year. Water consumption derives from 1336 wells having an annual discharge of 557.10 million m^3 and 23 Qanat systems with an annual discharge of 7.3 million m^3. Agriculture consumes 514.3 million m^3, drinking water comprises 36.9 million m^3,

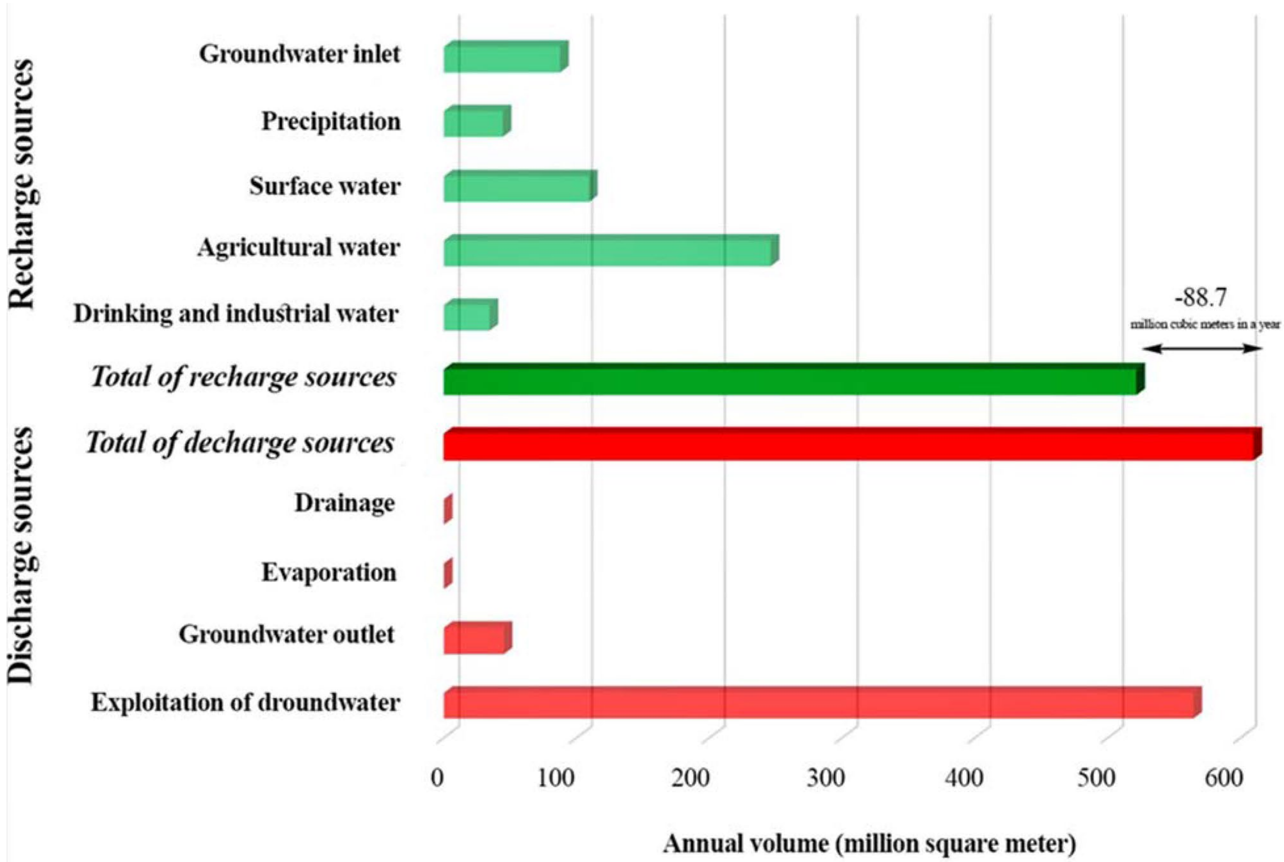

Fig. 3 Volume corresponding to each withdrawal and recharge components of the alluvial aquifer of Aliabad plain

and industrial use consumes 6.9 million m^3 (Office of Water and Abfa Operating and Protection Systems 2012).

Subsidence

Aliabad has been observed to experience subsidence in recent years as evidenced by exposed well casings and ground fissures in the plain (Qom Regional Water Company 2013). Without subsidence-monitoring tools, such as the global positioning system (GPS), and an insufficient number of piezometers in Aliabad plain, radar interferometry was chosen as the best alternative to monitoring land deformation and subsidence. This method offers extensive coverage, economic efficiency, and sufficient accuracy over broad areas. Sensory images from Sentinel-1 (ESA 2016) were used to detect land subsidence in the plain during 2015 and 2016 (Fig. 4) The area experienced maximum subsidence of 22 cm during the 506 days under study. The amount of subsidence was greater in the west than in the east (Edalat et al. 2020).

Aliabad aquifer groundwater modeling using GMS

The flow of water through the aquifer is usually described using differential equations. The following equation describes the 3D flow of groundwater in a porous medium under transient state conditions (Biot 1941) as:

$$\frac{\partial}{\partial x}\left(k_{xx}\frac{\partial h}{\partial x}\right)+\frac{\partial}{\partial y}\left(k_{yy}\frac{\partial h}{\partial x}y\right)+\frac{\partial}{\partial z}\left(k_{zz}\frac{\partial h}{\partial z}\right)=S_s\frac{\partial h}{\partial t}+R, \quad (1)$$

where k_{xx}, k_{yy}, and k_{zz} are hydraulic conductivity in the *x, y*, and *z* directions, respectively; *h* is the piezometric head, S_s is the specific storage, *R* is the storage period, and *t* is the time. The right side of the equation equals zero for steady-state conditions.

For simple scenarios, Eq. (1) can be solved using analytical methods (Chan et al. 1978). However, analytical methods cannot be used to solve complex systems; thus, numerical approaches have been used (Anderson and

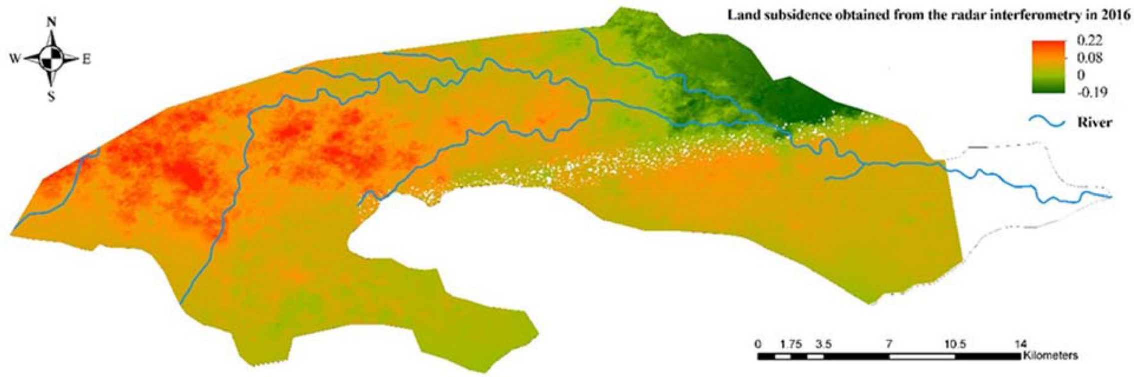

Fig. 4 Land deformation (m) of the study area obtained from InSAR data during 2015 to 2016 (Edalat et al. 2020)

Woessner 1992; McDonald and Harbaugh 1988). For complicated conditions that affect aquifers such as the hydrogeological boundaries and undefined geometry, numerical methods are used more often. MODFLOW software features the most applications for simulating groundwater flow and was developed by the United States Geological Survey (USGS). This software can model three-dimensional (3D) flow using the finite difference method (Karimi et al. 2019). GMS helps more powerful models such as MODFLOW simulate groundwater flow under complex hydrogeological conditions. Figure 5 shows the overall groundwater modeling steps.

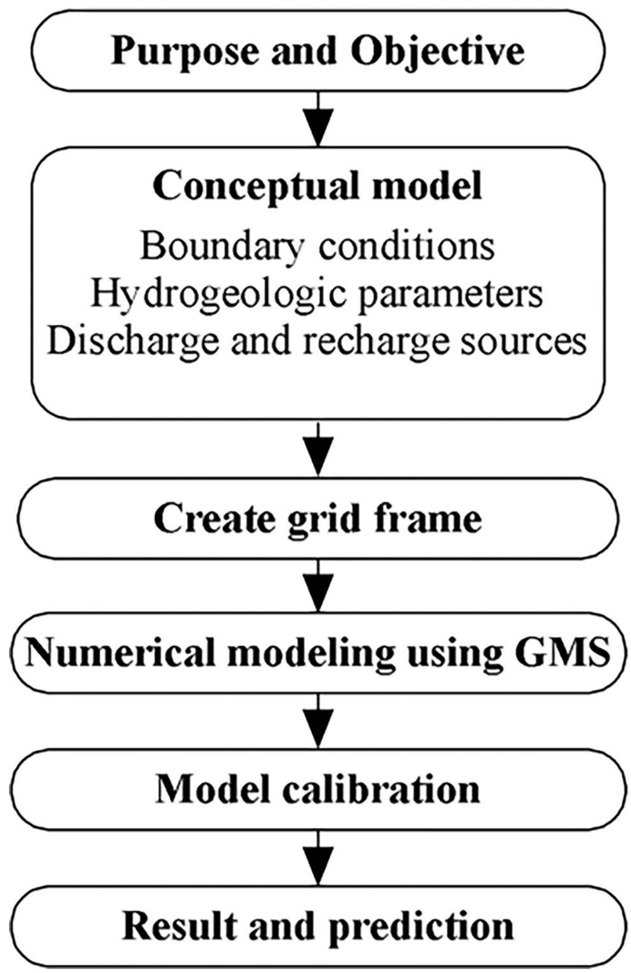

Fig. 5 Flowchart of groundwater modeling using GMS

Conceptual model

A conceptual model is the first crucial step of the modeling process that helps establish the boundary conditions for a numerical model of a system. In the current study, the conceptual model was generated by virtual coverage of the boundary conditions, hydrological parameters, and recharge and withdrawal origins. The hydraulic definition of the boundary conditions was used to solve the partial differential equations for the groundwater with the data available within the boundaries. Hence, after plotting the equipotential lines and investigating the geology of the area, the physical boundaries of the model were determined using the hydraulic heads of the natural state of the aquifer. Figure 6 shows the area boundaries, which were based on the level lines of the groundwater. The red lines in Fig. 6 are the permeable borders. The other boundaries of the study area were considered to be impermeable.

The hydraulic parameters include the coverage of hydraulic conductivity and specific discharge coefficients. The initial values for hydraulic conductivity (K) can be calculated as:

$$K = T/b, \tag{2}$$

where T and b are the transport capacity and sediment thickness, respectively. The specific discharge coefficient (S_Y) of Aliabad plain aquifer was considered to be 5% as the mean by taking into account the base of the aquifer (Demenico and Schwartz 1990).

The recharge sources of the aquifer are the groundwater, precipitation, and water intrusion from drinking water,

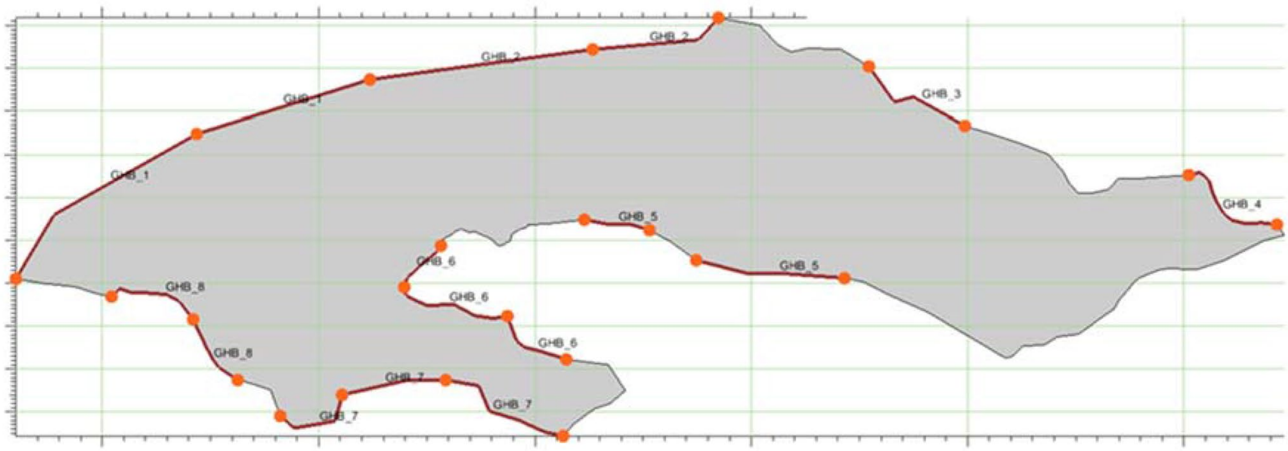

Fig. 6 Limits of permeable and impermeable borders of the study area

industry and agricultural origins. The discharge origins are exploitation wells, Qanats and fountains. The data for these origins have been provided by the regional water company (Qom Regional Water Company 2016).

Finite difference grid for the model

Once the conceptual model was created, the grid was constructed to fit the conceptual model. The number of rows and columns (and thus the number of cells) for the grid were determined to create a proper fit to the model. This affected the running time and accuracy of the model. The grid was made up of 43 rows and 129 columns. Of the total of 5547 cells, 2124 were active (blue cells in Fig. 7) and 3423 were inactive (red cells in Fig. 7). All cells were square in shape and were 600 × 600 m in size. Information available from the observation wells was used to establish the calibration time interval for the model of 120 months for the period from 2006 to 2016.

Calibration of steady and transient models

The hydraulic head data of the first year (2006) was used to simulate the steady-state model. To simulate the groundwater flow in the transient state, variations in the time parameters for the model were defined. To do this, the hydraulic head changes that were measured between 2006 and 2016 were used. After executing the primary model with the proposed states, large errors were expected because of the uncertainty of the input parameters. To minimize the error in the results during calibration, the input parameters of the groundwater model were modified. This process continued until the model output matched the observed dataset. In this step, hydraulic conductivity was modified during calibration. The model was adjusted such that the difference between the observed and

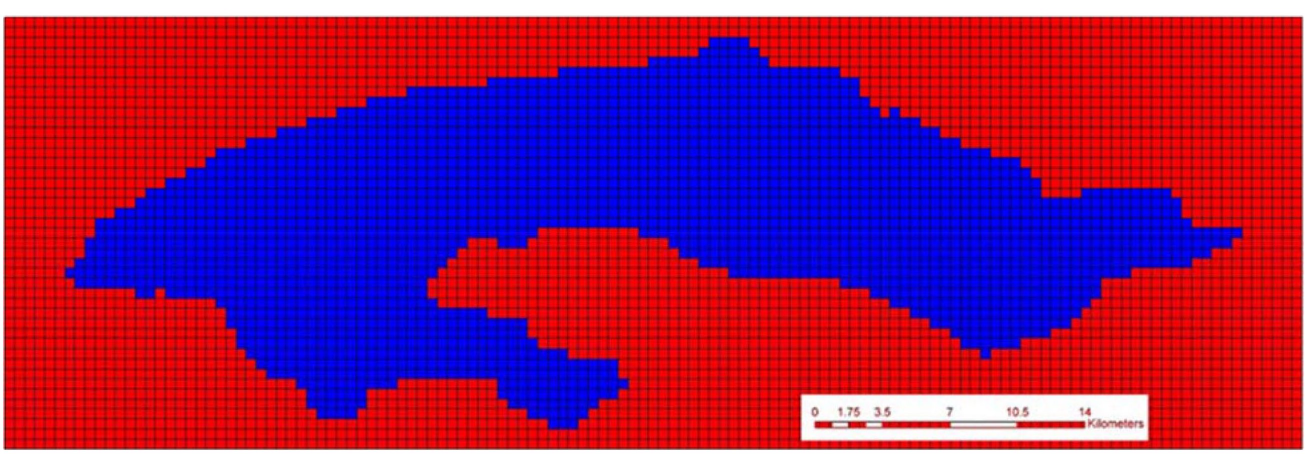

Fig. 7 Location of the studied region in Aliabad plain and networking of this region

simulated hydraulic head for each piezometric well decreased to a reasonable value. For this purpose, the hydraulic heads data from the 26 observation wells were used (Fig. 1).

Several approaches are available for minimizing error during calibration. One simple method is the use of trial-and-error method. Although this method is easy to use, it may not produce a reasonable conceptual output. More complicated methods have used mathematical techniques to minimize calibration error. One of these is the parameter estimation (PEST) method. This method estimates goal parameters and aids in data interpretation, model calibration, and analysis of predictions (Aquaveo 2017). In this study, the PEST tool was used with the pilot method to calibrate the hydraulic conductivity.

After the groundwater levels for the 2006–2016 period were calculated in the model, the values were compared with the actual values measured in the observation wells. Common statistical methods such as root mean square error (RMSE), index of agreement (d) (Willmott and Wicks 1980) and the Nash–Sutcliffe coefficient of efficiency (NSE) (Nash and Sutcliffe 1970) were used in the following equations:

$$\mathrm{RMSE} = \sqrt{\frac{\sum_{i=1}^{n}(Y_i^{\mathrm{obs}} - Y_i^{\mathrm{sim}})^2}{n}}, \tag{3}$$

$$d = 1 - \left[\frac{\sum_{i=1}^{n}(Y_i^{\mathrm{obs}} - Y_i^{\mathrm{sim}})^2}{\sum_{i=1}^{n}\left(\left|Y_i^{\mathrm{obs}} - Y_i^{\mathrm{sim}}\right| + \left|Y_i^{\mathrm{obs}} - Y_i^{\mathrm{mean}}\right|\right)^2}\right], \tag{4}$$

$$\mathrm{NSE} = 1 - \left[\frac{\sum_{i=1}^{n}(Y_i^{\mathrm{obs}} - Y_i^{\mathrm{sim}})^2}{\sum_{i=1}^{n}(Y_i^{\mathrm{obs}} - Y_i^{\mathrm{mean}})^2}\right], \tag{5}$$

where Y^{obs} is the observed value of the head, Y^{sim} is the predicted value of the head, Y^{mean} is the observed amount of data and n is the number of observations. RMSE is a non-negative value that approaches zero when modeling is accurate. The index of agreement varies between 0 and 1, where 1 denotes better agreement. NSE varies between $-\infty$ and 1, with the higher values denoting accuracy of the model.

Figure 8 shows the calculated and observed groundwater levels from 26 piezometers in the area of interest. Reasonable agreement is evident between the observed and calculated values and the RMSE error corresponding to the 120 time-steps of modeling is equal to 1.4. Table 1 lists the RMSE, d, and NSE values for each piezometer used to assess the total accuracy of the mean difference between the observed and calculated values. These parameters were in the acceptable range for all observation wells. The difference in the mean groundwater level between the observed and calculated values in 13 piezometers was less than 0.5 m. The maximum mean difference between the calculated and observed values was 2.94 m for piezometer 8. This value corresponded to changes in the groundwater level (810–930 m) and indicates a modeling error of 2.5% and a total modeling accuracy of 97.5%.

Subsidence aquifer SUB

After calibrating the model and obtaining results that met generally accepted calibration criteria, the elastic (reversible) and inelastic (irreversible) deformations of sediments in the aquifer was simulated by SUB. Changes in the effective stress in the saturated zone of an unconfined aquifer can be described as:

$$\Delta\sigma'_{zz} = -\rho_w g\left(1 - n + n_w\right)\Delta h, \tag{6}$$

where $\Delta\sigma'_{zz}$, is the change in effective stress, n_w is the porosity of the aquifer, and Δh is change in the hydraulic head and $\rho_w g$ is the moisture content (as a percentage of saturation)

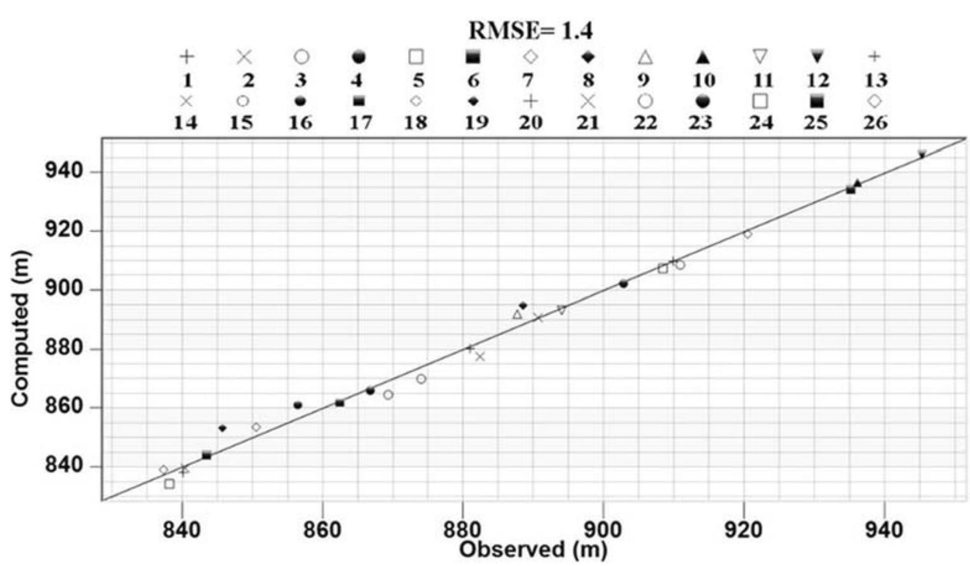

Fig. 8 Agreement level of the observed and calculated heads in 26 piezometers of the study area

Table 1 The mean difference between observed and calculated water levels, RMSE, *d*, and NSE in 26 piezometers of the study area

Piezometer number	Mean difference between observed and calculated water levels (m)	RMSE	*d*	NSE	Piezometer number	Mean difference between observed and calculated water levels (m)	RMSE	*d*	NSE
1	0.26	0.31	0.99	0.99	14	2.00	2.32	0.55	0.62
2	0.41	0.49	0.86	0.92	15	2.22	2.59	0.56	0.67
3	2.36	2.57	0.99	0.59	16	1.66	2.01	0.72	0.87
4	0.31	0.37	0.84	0.90	17	0.37	0.46	0.97	0.97
5	0.48	0.56	0.4	0.64	18	1.76	1.87	0.76	0.88
6	0.43	0.51	0.37	0.65	19	1.49	1.77	0.66	0.86
7	0.39	0.61	0.39	0.67	20	1.27	1.45	0.71	0.86
8	2.94	3.40	0.006	0.72	21	0.34	0.41	0.99	0.99
9	2.71	3.16	0.60	0.64	22	2.16	2.59	0.23	0.30
10	0.18	0.26	0.001	0.71	23	0.43	0.51	0.34	0.60
11	0.33	0.42	0.007	0.43	24	2.05	2.28	0.72	0.87
12	0.29	0.34	0.13	0.61	25	1.64	1.78	0.80	0.90
13	2.50	3.09	0.20	0.77	26	0.46	0.60	0.69	0.87

in the unsaturated zone. In a confined aquifer, the change in effective stress is defined as:

$$\Delta\sigma'_{zz} = -\rho_w g \Delta h. \quad (7)$$

SUB is based on Eq. (7) and simulates the compaction and changes of storage in confined aquifers. For the saturated zone of an unconfined aquifer, compaction and changes of storage is calculated using Eq. (6) (Hoffmann et al. 2003).

Results and discussion

Trend of groundwater exploitation from aquifer

The calibrated and validated transient model was used to predict the changing trends of the aquifer in the 10-year period to 2026 to forecast the future conditions in the study area. Three scenarios were predicted based on variations in the exploitation flow. The first scenario was to maintain the conditions during the last year of modeling. The second and third scenarios involved a 10% and 30% decrease in groundwater exploitation, respectively. Figure 9 presents the aquifer hydrograph of Saveh plain under the three scenarios. As seen, a 10% decrease in pumping caused depletion of the aquifer and stabilization of the descending trend in the aquifer hydrograph. The 30% decrease caused aquifer hydrograph to ascend in the long term. Even with the assumption of expansion of drought and a decrease in the recharge sources of groundwater, also caused by illegal well drilling, a 30% decrease in aquifer exploitation could reverse the declining trend of the hydrograph into an ascending trend. Since a short-term decrease in the exploitation level of 30% is not possible to achieve, artificial charging of the aquifers must be developed in an efficient location.

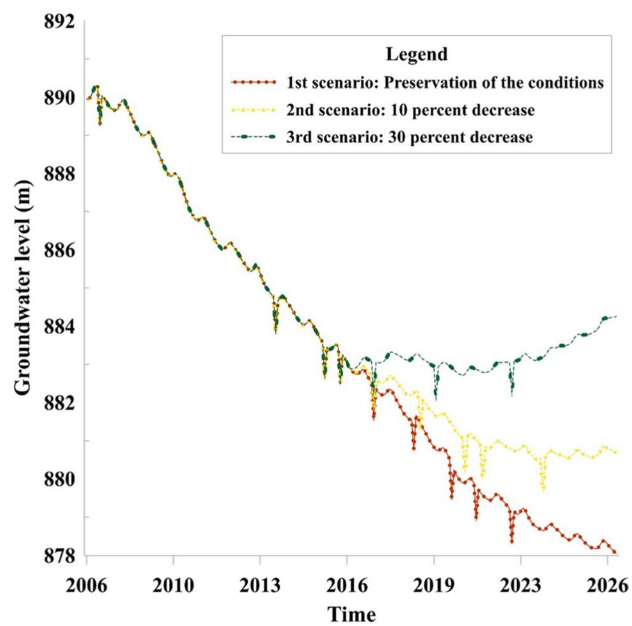

Fig. 9 Aquifer hydrograph of Saveh plain under three scenarios between the years 2006 and 2026

Model of subsidence under groundwater exploitation

The geometry of subsidence in the area of interest was a result of the validated model at the end of the modeling period (2016) as shown in Fig. 10a. In this figure, the maximum subsidence predicted in the study area was 35 cm. A comparison of the geometric distribution of subsidence with radar interferometry results (Fig. 4) shows that the model results correctly predicted the region with maximum subsidence as being in the western part of the area. However, the subsidence distribution predicted by the model differed from the results of radar interferometry, especially in the west.

The difference could be explained in one of three ways. The first option is the unavailability of land deformation data at the onset of modeling (2006); thus, this value was assumed to be zero. The second is that subsidence as modeled for the 2006–2016 period, but radar images of subsidence were for the years 2015 and 2016. The third involves factors such as agricultural activity, the influence of seasonal changes, and the locational distribution of subsidence from radar interferometry. The model predictions of subsidence assume that the current rate of groundwater exploitation also applies in 2026 is shown in Fig. 10b. As seen, preserving the current rate of exploitation would lead to subsidence at more sites on the plain, and the maximum subsidence of the plain would reach 47 cm.

Figure 11 shows the effects of scenarios involving a decrease in groundwater exploitation on the average subsidence in the study area up to 2026. As seen, land subsidence was strongly linked to the decline of the groundwater level hydrographs (Fig. 9). If the current critical rate of exploitation is maintained, the rate of increase in subsidence (blue curve in Fig. 11) will progress to a level at which most parts of the aquifer will be damaged. In the final months of the prediction period, although the subsidence graph shows a milder trend, this is not a sign of improvement. On the contrary, it indicates that the full potential of the aquifer has been greatly decreased and aquifer porosity has been greatly reduced.

The red curve in Fig. 11 indicates land deformation for a 10% decrease in aquifer exploitation. At the 10% decrease in the exploitation rate, subsidence continues to increase, but the rate of increase would be reduced by comparison with the first scenario. In the third scenario (green curve in Fig. 11), it is predicted that a 30% decrease in aquifer exploitation could halt subsidence only when the other parameters of the model are preserved. The results indicate that none of these scenarios can reverse the descending trend of the subsidence graph into an ascending trend. In such a case, land subsidence in the study area could be reversed. With the

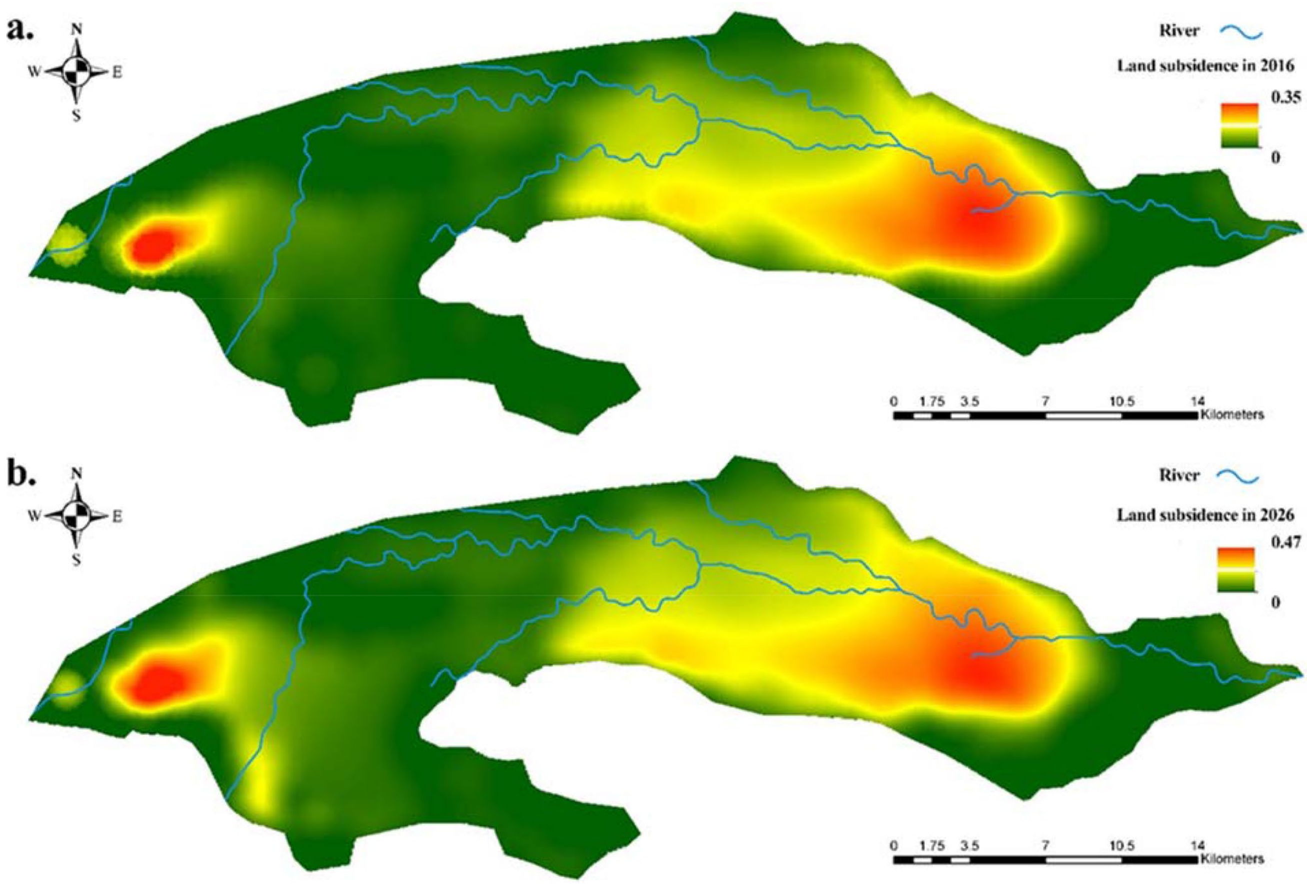

Fig. 10 **a** Model prediction of the subsidence in the year 2016 and **b** model prediction of subsidence in the year 2026

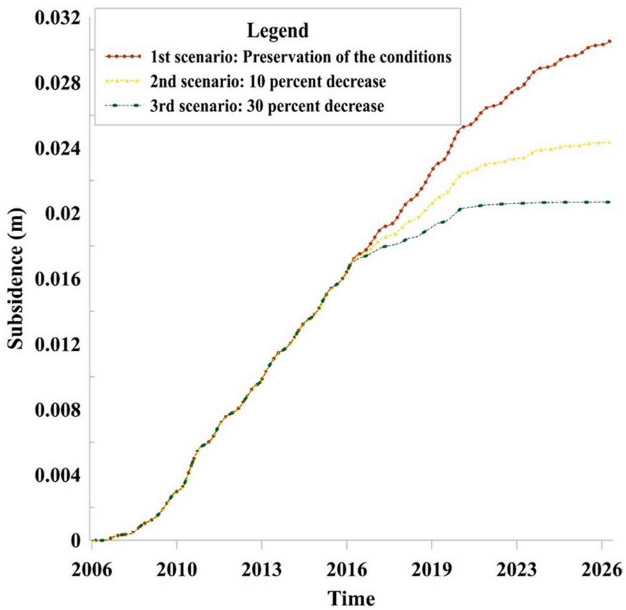

Fig. 11 Time changes of the average value of subsidence in the study area under three prediction scenarios

heavy demands of the agricultural economy for groundwater resources, immediate action must be taken develop rigorous preservation and stabilization plans.

Conclusions

The present study modeled the groundwater levels in the Aliabad plain aquifer in Qom province in central Iran for the period of 2006–2016. GMS software was used with the MODFLOW architecture to develop a model for estimating how the hydraulic heads in the aquifer varied spatially and over time in response to variations in groundwater abstraction and rainfall. To validate the model, the predicted values for the hydraulic head were compared with the observed values from observation wells. The results show adequate agreement between the observed and calculated values. The RMSE error for 120 time-steps of modeling was 1.4. In 13 out of 26 piezometers, the maximum mean difference between the calculated and observed groundwater levels was less than 50 cm. The maximum mean difference between the observed and calculated values was 2.94 and occurred at piezometer 8. These values show an acceptable modeling error of 2.5% for groundwater level variations of between 810 and 930 m in altitude.

The validation results indicate that MODFLOW mathematical model converged, ran, and calibrated well for groundwater flow simulation. Consequently, this modeling approach could be used as a management tool for other areas with similar geological and hydrological conditions. Scenarios of decrease in the exploitation level evaluated the hydrograph response of the aquifer to 10% and 30% reductions in exploitation. The results showed that a 30% reduction in exploitation could halt the descending trend of the hydrograph in the long term and reverse it to an ascending trend.

Land subsidence also was modeled after the optimal definitions were established for the basic coefficients using SUB. Results of the land subsidence model successfully predicted maximum subsidence of 35 cm in 2016.

A comparison of the predicted spatial distribution of subsidence with land deformation results that were obtained from radar interferometry indicated that the modeling results in this research successfully predicted the location of maximum subsidence. The results of the land subsidence predictions up to 2026 show that if the current rate of exploitation of groundwater is held constant, the study area will experience a maximum subsidence of 47 cm. Examination of three scenarios for the rate of land subsidence (holding current rate constant, a 10% decrease, and a 30% decrease in exploitation) indicates that vertical land elevation change is directly related to a decrease in groundwater levels. The results also show that although strict aquifer stabilization plans can help reduce aquifer vulnerability, they will not be able to reverse the conditions related to land subsidence.

References

Amighpey M, Arabi S (2016) Studying land subsidence in Yazd province Iran, by integration of InSAR and levelling measurements. Remote Sens Appl Soc Environ. https://doi.org/10.1016/j.rsase.2016.04.001

Anderson MP, Woessner WW (1992) The role of the postaudit in model validation. Adv Water Resour 15:167–173

Aquaveo (2017) GMS 10.3 Tutorials Environmental Modeling Research Laboratory. Brigham Young University, Provo

Bajni G, Apuani T, Beretta GP (2019) Hydro-geotechnical modelling of subsidence in the Como urban area. Eng Geol 257:105144. https://doi.org/10.1016/j.enggeo.2019.105144

Bakker M, Hemker K (2004) Analytic solutions for groundwater whirls in box-shaped, layered anisotropic aquifers. Adv Water Resour 27:1075–1086

Bell JW (1981) Subsidence in Las Vegas Valley. University of Nevada, Mackay School of Mines, Reno

Biot M (1941) The general three-dimensional consolidation theory. J Appl Phys 12:155–164

Budhu M (2011) Earth fissure formation from the mechanics of groundwater pumping. Int J Geomech 11:1–11

Chan Y, Mullineux N, Reed J, Wells G (1978) Analytic solutions for drawdowns in wedge-shaped artesian aquifers. J Hydrol 36:233–246

Chiang W-H (2005) 3D-Groundwater modeling with PMWIN: a simulation system for modeling groundwater flow and transport processes. Springer Science & Business Media, Berlin

Cui Y, Su C, Shao J, Wang Y, Cao X (2014) Development and application of a regional land subsidence model for the plain of Tianjin. J Earth Sci 25:550–562

Dehghani M, Valadan Zoej MJ, Hooper A, Hanssen RF, Entezam I, Saatchi S (2013) Hybrid conventional and Persistent Scatterer SAR interferometry for land subsidence monitoring in the Tehran Basin. Iran. ISPRS J Photogramm Remote Sens 79:157–170. https://doi.org/10.1016/j.isprsjprs.2013.02.012

Demenico P, Schwartz F (1990) Physical and chemical hydrogeology. Wiley, New York

Diersch H (2005) FEFLOW finite element subsurface flow and transport simulation system. Institute for Water Resources Planning and System Research, Berlin

Edalat A, Khodaparast M, Rajabi AM (2020) Detecting land subsidence due to groundwater withdrawal in Aliabad plain, Iran, using ESA Sentinel-1 satellite data. Nat Resour Res 29:1935–1950. https://doi.org/10.1007/s11053-019-09546-w

ESA (2016) Sentinel-1 scientific data hub. European Space Agency. Available at: https://scihub.copernicus.eu/dhus

Galloway DL, Burbey TJ (2011) Review: Regional land subsidence accompanying groundwater extraction. Hydrogeol J 19:1459–1486. https://doi.org/10.1007/s10040-011-0775-5

Hoffmann J, Leake SA, Galloway DL, Wilson AM (2003) MODFLOW-2000 ground-water model—user guide to the subsidence and aquifer-system compaction (SUB) package. Geological Survey, Washington DC

Hu L et al (2019) Land subsidence in Beijing and its relationship with geological faults revealed by Sentinel-1 InSAR observations. Int J Appl Earth Obs Geoinf 82:101886. https://doi.org/10.1016/j.jag.2019.05.019

Karimi L, Motagh M, Entezam I (2019) Modeling groundwater level fluctuations in Tehran aquifer: results from a 3D unconfined aquifer model. Groundwater Sustain Dev 8:439–449

Karimipour AR, Rakhshanderoo G (2011) Sensitivity analysis for hydraulic behavior of Shiraz plain aquifer using PMWIN. Water Wastewater 22:102–111

Konikow LF, Kendy E (2005) Groundwater depletion: A global problem. Hydrogeol J 13:317–320

Lashkaripour GR, Ghafoori M (2011) The effects of water table decline on the groundwater quality in aquifer of Torbat Jam Plain, Northeast Iran. Int J Emerg Sci 1:153–163

Ma P, Wang W, Zhang B, Wang J, Shi G, Huang G, Chen F, Jiang L, Lin H (2019) Remotely sensing large- and small-scale ground subsidence: a case study of the Guangdong-Hong Kong–Macao Greater Bay Area of China. Remote Sens Environ 232:111282. https://doi.org/10.1016/j.rse.2019.111282

Mahdavi M, Farokhzadeh B, Salajegheh A, Malakian A, Souri M (2013) Simulation of Hamedan-Bahar aquifer and investigation of management scenarios by using PMWIN. Whatershed Manag Res 26:108–116

Mahmoudpour M, Khamehchiyan M, Nikudel M, Ghassemi M (2016) Numerical simulation and prediction of regional land subsidence caused by groundwater exploitation in the Southwest Plain of Tehran, Iran. Eng Geol 201:6–28. https://doi.org/10.1016/j.enggeo.2015.12.004

McDonald MG, Harbaugh AW (1988) A modular three-dimensional finite-difference ground-water flow model. US Geological Survey, Reston

Moe IR, Kure S, Januriyadi NF, Farid M, Udo K, Kazama S, Koshimura S (2017) Future projection of flood inundation considering land-use changes and land subsidence in Jakarta, Indonesia. Hydrol Res Lett 11:99–105

Motagh M, Djamour Y, Walter TR, Wetzel H-U, Zschau J, Arabi S (2007) Land subsidence in Mashhad Valley, northeast Iran: results from InSAR, levelling and GPS. Geophys J Int 168:518–526. https://doi.org/10.1111/j.1365-246X.2006.03246.x

Nash JE, Sutcliffe JV (1970) River flow forecasting through conceptual models part I—a discussion of principles. J Hydrol 10:282–290

Office of Water and Abfa Operating and Protection Systems (2012) Groundwater balancing program. Ministry of Energy, Deputy Minister of Water and Abfa, Delhi

Qin H, Andrews CB, Tian F, Cao G, Luo Y, Liu J, Zheng C (2018) Groundwater-pumping optimization for land-subsidence control in Beijing plain, China. Hydrogeol J 26:1061–1081

Qom Regional Water Company (2000) Geophysical studies of Qom province. Ministry of Energy, Iran Water Resources Management Company, Tehran

Qom Regional Water Company (2013) Water resources report of Saveh study area Abkhan consulting engineers. Ministry of Energy, Iran Water Resources Management Company, Tehran

Qom Regional Water Company (2016) Information on observation wells and exploitation wells in Aliabad plain of Qom (4112 study area). Ministry of Energy, Iran Water Resources Management Company, Tehran

Rahnama MB, Moafi H (2009) Investigation of land subsidence due to groundwater withdraw in Rafsanjan plain using GIS software. Arab J Geosci 2:241–246. https://doi.org/10.1007/s12517-009-0034-4

Rajabi AM (2018) A numerical study on land subsidence due to extensive overexploitation of groundwater in Aliabad plain, Qom-Iran. Nat Hazards 93:1085–1103. https://doi.org/10.1007/s11069-018-3448-z

Rajabi AM, Ghorbani E (2016) Land subsidence due to groundwater withdrawal in Arak plain, Markazi province, Iran. Arab J Geosci 9:738

Regli C, Rauber M, Huggenberger P (2003) Analysis of aquifer heterogeneity within a well capture zone, comparison of model data with field experiments: a case study from the river Wiese, Switzerland. Aquat Sci 65:111–128

Rodolfo KS, Siringan FP (2006) Global sea-level rise is recognised, but flooding from anthropogenic land subsidence is ignored around northern Manila Bay, Philippines. Disasters 30:118–139

Terzaghi K (1925) Principles of soil mechanics, IV—Settlement and consolidation of clay. Eng News Rec 95:874–878

Willmott CJ, Wicks DE (1980) An empirical method for the spatial interpolation of monthly precipitation within California. Phys Geogr 1:59–73